Archives of Biochemistry and Biophysics 478 (2008) 119–126

Contents lists available at ScienceDirect

Archives of Biochemistry and Biophysics

journal homepage: www.elsevier.com/locate/yabbi

Tau-isoform dependent enhancement of taxol mobility through microtubules

HyunJoo Park [a,b,*], MahnWon Kim [a,1], Deborah K. Fygenson [b,2]

[a] Physics Department, Korea Advanced Institute of Science and Technology, Daejeon 305-701, Republic of Korea
[b] Physics Department and Biomolecular Science and Engineering Program, University of California, Santa Barbara, CA 93106, USA

ARTICLE INFO

Article history:
Received 1 June 2008
and in revised form 17 July 2008
Available online 26 July 2008

Keywords:
Fluorescence recovery after photobleaching (FRAP)
Microtubules
Microtubule-associated protein
Tau
Rebinding
Kinetic modeling
Transport though pores
Competition

ABSTRACT

Tau, a family of microtubule-associated proteins (MAPs), stabilizes microtubules (MTs) and regulates their dynamics. Tau isoforms regulate MT dynamic instability differently: 3-repeat tau is less effective than 4-repeat tau at suppressing the disassembly of MTs. Here, we report another tau-isoform-dependent phenomenon, revealed by fluorescence recovery after photobleaching measurements on a BODIPY-conjugated taxol bound to MTs. Saturating levels of recombinant full-length 3-repeat and 4-repeat tau both cause taxol mobility to be remarkably sensitive to taxol concentration. However, 3-repeat tau induces 2.5-fold faster recovery (~450 s) at low taxol concentrations (~100 nM) than 4-repeat tau (~1000 s), indicating that 3-repeat tau decreases the probability of taxol rebinding to its site in the MT lumen. Finding no tau-induced change in the MT-binding affinity of taxol, we conclude that 3-repeat tau either competes for the taxol binding site with an affinity of ~1 μM or alters the MT structure so as to facilitate the passage of taxol through pores in the MT wall.

© 2008 Elsevier Inc. All rights reserved.

The microtubule (MT)[3] is a hollow, crystalline assembly of the heterodimeric α,β-tubulin protein and the stiffest element of the cellular skeleton [1]. Many important cellular functions of MTs, including mitosis and locomotion, depend on the regulation of dynamic instability by microtubule-associated proteins (MAPs) [2]. Tau is one of several MAPs that stabilize MT dynamics. Tau has received a great deal of attention since it was discovered to be the major constituent of neurofibrillary tangles that are the hallmark of a variety of neurodegenerative diseases [3–5]. The prospect of clarifying the origins of these diseases motivates much research into the mechanism of tau's MT-stabilizing effect.

Tau is a soluble and natively unfolded polypeptide in solution [6,7] that acquires structure as it binds the microtubule [8]. Its MT-binding domain contains either three or four conserved repeat sequences, strongly suggesting that a single molecule of tau bridges multiple dimers in the MT lattice [9]. Exactly where tau binds on the MT exterior remains to be resolved [10–12]. Recent experiments indicate that tau can also bind to the MT interior, at a location on near β-tubulin that overlaps the binding site for taxol [13].

Taxol is a small, hydrophobic molecule that has proven to be an effective therapeutic for certain cancers due to its MT-stabilizing properties [14,15]. MT-mediated interactions between taxol and tau may point to a common mechanism of MT stabilization, which could shed light on the mechanism of MT dynamics as well as improve clinical protocols. To date there are four types of evidence: (i) taxol displaces weakly bound tau from MTs *in vitro* [13]; (ii) taxol mobility becomes sensitive to taxol concentration in tau-saturated MTs *in vitro* [16]; (iii) taxol causes detachment of tau from MTs *in vivo* [17]; and (iv) taxol restores tau-linked functions, like axonal transport, in neurodegenerative thauopathies [18].

Given that different isoforms of tau have different effects on MT dynamics both *in vitro* and *in vivo* [19,20], it is natural to ask whether the interaction between taxol and tau evidenced above is isoform-specific. Evidence of type (i) reveals differences that correlate most strongly with the presence or absence of one of the conserved peptide repeats and its adjoining sequence in the C-terminal half of the protein [13].

Here, we document yet another isoform-specific effect of tau on MTs by studying the mobility of taxol. These experiments use a taxol analog with a fluorescent label and measure fluorescence recovery after photobleaching (FRAP) on tau-decorated MTs. The results reveal a significant quantitative and qualitative difference between isoforms with three (3rTau) or four (4rTau) of the C-terminal repeats. At low taxol concentrations, 3rTau speeds taxol's recovery nearly 2.5-fold, while 4rTau has no discernable effect.

To interpret this result, we model how recovery relates to taxol-binding kinetics using a first-order reaction scheme. The model

* Corresponding author. Address: Physics Department, Korea Advanced Institute of Science and Technology, Daejeon 305-701, Republic of Korea. Fax: +82 42 869 8150.
E-mail addresses: phj78@kaist.ac.kr (H. Park), mwkim@kaist.ac.kr (M. Kim), deborah@physics.ucsb.edu (D.K. Fygenson).
[1] Fax: +82 42 869 8150.
[2] Fax: +1 805 893 3307.
[3] *Abbreviations used:* MT, microtubule; MAPs, microtubule-associated proteins.

0003-9861/$ - see front matter © 2008 Elsevier Inc. All rights reserved.
doi:10.1016/j.abb.2008.07.020

motivates further experiments, which rule out explanations based on a tau-dependent change in the MT-binding affinity of taxol or changes in the large-scale structure of the MTs. We conclude that 3rTau interferes locally with the accessibility of the taxol site for re-binding and discuss possible mechanisms.

Materials and methods

Tau

Recombinant full-length adult human brain 3-repeat tau and 4-repeat tau were the kind gifts of Dr. Stuart Feinstein (University of California, Santa Barbara). Both were purified by the procedures described in [20] from Rosetta (DE3) pLacI cells induced with 1 mM isopropyl-β-D-thiogalactoside. Stock tau concentrations were determined by the Bradford assay in comparison with a tau standard. The latter was established by SDS–PAGE and Coomassie blue staining (Pierce, Rockford, IL) against a primary tau standard, calibrated by mass spectrometry.

Stock tau solutions were stored at −20 °C in BRB-80 buffer (80 mM Pipes, pH 6.8, 1 mM EGTA, 1 mM $MgSO_4$ and 10% β-mercaptoethanol) and then kept for 10 min at room temperature and vortexed before use.

Microtubules and taxol with tau

Microtubules (MTs) were prepared by first mixing 5 μL of 5 mg/mL bovine brain tubulin (Cytoskeleton, Denver, CO) with 4 mg/mL 110 kDa dextran (Pharmacia, Uppsala, Sweden) in G-PEM buffer (1 mM GTP, 100 mM Na-Pipes, 1 mM EGTA, 2 mM $MgCl_2$, 5% (w/w) glycerol, pH 6.8) and then incubating for 20 min at 37 °C. These assembly conditions are known to yield well-formed MTs [21], as we verified by TEM (see below).

Red-orange fluorescent BODIPY® 564/570 paclitaxel (Molecular Probes, Eugene, OR), here in referred to as *botax*, was hydrated in 100% dimethylsulfoxide (DMSO) to a stock concentration of 100 μM. To keep DMSO at less than 10% in the final solution, the highest concentration of free taxol, 5 μM, was made using 75% unlabeled taxol (Sigma, St. Louis, MO) and 25% botax. Botax was diluted in G-PEM with 4 mg/mL 110 kDa dextran before being added to the MT samples, which were incubated again at the same temperature for the same amount of time. (Addition of botax was calculated to result in the desired concentration ($100 - 10^4$ nM) free in solution [22] and later verified *in situ* as described below.)

Lastly, 3rTau was mixed with the botax–MT solution to yield a molar ratio of either 1:3 or 1:1 tau-to-tubulin, the resulting solution was again incubated for 20 min at 37 °C. In all cases, the final concentration of tubulin was 2.5 mg/ml (~22.7 μM).

Fluorescence recovery after photobleaching (FRAP)

Briefly, inside a flow cell made of a coverslip, slide and parafilm gasket, melted G75 Sephadex beads (Sigma, St. Louis, MO) stick to the slide and swell to an average size of 40–120 μm when wet. Sample solution is inserted using capillary flow and MTs collect and align around the Sephadex beads. The botax bound to aligned MTs loses its fluorescence (bleaches) when exposed to focused light from a mercury arc lamp (100 W).

During FRAP, epifluorescence images were recorded every few decimal seconds using a shutter (Uniblitz, Rochester, NY) to avoid unnecessary bleaching. Taxol (size ~1 nm) is small enough to diffuse freely through pores in the beads. MTs (diameter ~25 nm) are excluded. The concentration of free botax was determined to within ±26% by measuring the fluorescence intensity *in situ* at the center of a bead, 20 μm above the coverslip, using a cooled CCD camera (Cooke Corp, Romulus, MI) and comparing to standard botax solutions in a similar flow cell without MTs (50–5000 nM).

Images were analyzed using ImageJ (NIH, ver. 1.32j). First, a circular region-of-interest (ROI) was selected around the bleached spot. Then, mean intensity outside the ROI was subtracted from the mean intensity inside the ROI, to correct for any bleaching during data collection, and plotted against time. All plots were well fit by a single exponential

$$I(t) = (I_\infty - I_o) \cdot \exp(-t/\tau_R) \quad (1)$$

where I_∞ represents the amplitude at infinite time, I_o is the amplitude difference between $t = 0$ and infinite time and τ_R is the recovery time (Fig. 1).

In these experiments, the signal is dominated by bound botax. Diffusion of free botax is not directly observed because the fluorescence intensity of botax increases dramatically upon binding to MTs (see Results).

Microtubule bundles

Early experiments, performed without Tau, demonstrated that botax recovery was very sensitive to the density of aligned MTs [22]. The presence of even a small amount of tau (e.g., 1:50 molar ratio with tubulin) separates aligned MTs and results in recovery times that are reproducible throughout a given sample [16].

It has been suggested that the separation between aligned MTs may be due to stiff tau–tau cross-bridges that form between microtubules [23]. We checked, however, that in the absence of dextran, flow-aligned MTs appear equally diffuse with or without full-length 3rTau (Fig. 2). This observation, that tau alone does not compactify MTs, supports the hypothesis that the N-terminal domains mediate a purely repulsive interaction under our conditions and, like bristles in a polymer brush, separate MTs via their time-averaged steric hindrance [24].

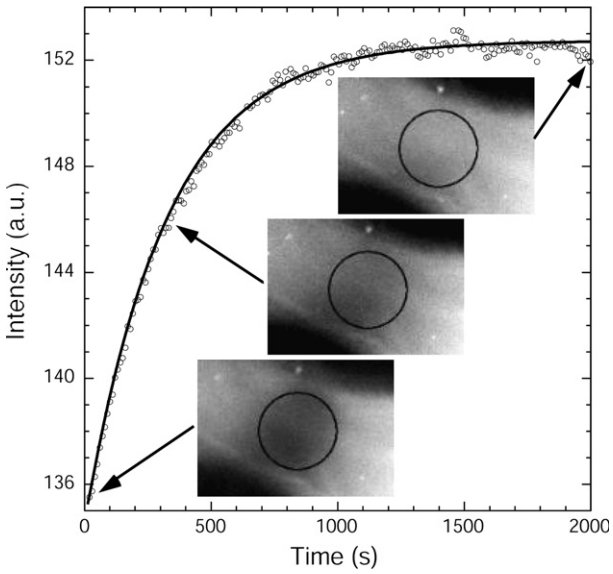

Fig. 1. Mean intensity (open circles) vs. time in a region-of-interest (ROI) that includes the bleached spot on a microtubule bundle around sephadex beads (dark area). The data fit a single exponential (solid line) of the form, $I(t) = I_\infty - I_0 \exp(-t/\tau_R)$. For this sample (300 nM botax, 2.5 mg/ml tubulin and 1:1 3rTau:tubulin), the recovery time τ_R is 331 ± 8 s. Images exemplify the raw data.

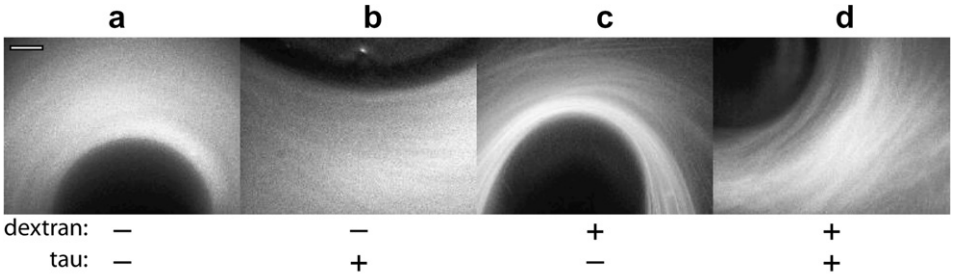

Fig. 2. Microtubules fluorescently labeled with botax and flow-aligned around sephadex beads (a) without both 110 kDa dextran (−) and 3rTau (−), (b) without dextran (−) but with 1:3 molar ratio of 3rTau to tubulin (+), (c) with dextran (+) but without 3rTau (−) and (d) with both dextran (+) and 1:3 3rTau (+).

Fluorimetry

Fluorimetry was performed in 40 μL quartz cuvettes (Starna, Atascadero, CA) using a fluorescence spectrophotometer (Cary Eclipse, Palo Alto, CA) set to an excitation wavelength of 540 nm and scanning the detection wavelength from 550 to 600 nm, using 5-nm slits in both light paths and 1 nm/s scan rate. The photomultiplier detector tube was set to 500 V.

Comparison of fluorescence emission from free botax and MT-bound botax was made using two 50-μL samples of 5 μM botax in G-PEM with 4 mg/ml 110 kDa dextran, one with and one without 20 μM polymerized tubulin.

Measurements of botax displacement by unlabeled taxol or 3rTau, were made using 50 μL samples of 5 μM botax and 20 μM polymerized tubulin in G-PEM with dextran, to which 2.3 μL of either 1100 μM unlabled taxol or 167 μM 3rTau (1:3 tau-to-tubulin) was added (yielding final concentrations of 4.8 μM botax, 19 μM tubulin and 48 μM taxol or 7.3 μM tau).

Transmission electron microscopy

MTs with or without botax and with or without full-length isoforms of either 3r or 4rTau were prepared in the same way as for FRAP and sedimented at 16,000*g* for 1 h. MT pellets were fixed for 1 h at room temperature in 2% glutaraldehyde, post-fixed for another 1 h with 1% osmium tetraoxide in BRB 80 and then stained overnight in 1% aqueous uranyl acetate. Fixed MT samples were dehydrated with acetone (25%, 50%, 75% and 100%), embedded in Spurr's resin (Polyscience Inc., Niles, IL) and incubated for 2 days at 80 °C. All embedded pellets were sectioned into 100-nm-thick slices on an ultramicrotome. Transmission electron microscopy (TEM) on these thin-sections was done on a JEM-12330 (JEOL Ltd., Japan) operating at 80 kV. Images were taken at 80,000× magnification. Over 800 MTs were counted for each condition and classified as close tubes, hooked tubes, open tubes or bowties.

Results and discussion

The possibility that the MT-mediated interference between taxol and tau might be tau-isoform-specific was most strongly suggested by the existence of tau-isoform-dependent influences on MT dynamic instability [13,19,20]. Because the interaction is predicated on microtubule binding, we focused on tau isoforms that differ in their C-terminal binding domain. Here, we report an isoform-specific effect of tau on the mobility of botax (a fluorescent analog of taxol) among tau-decorated MTs using fluorescence recovery after photobleaching (FRAP).

FRAP measures botax mobility

Our FRAP measures the amount of fluorescent botax bound to MTs in a region of interest over time. Because the fluorescence signal of free botax is overwhelmed by that of bound botax, the recovery displays single-exponential kinetics with a characteristic time, τ_R (Fig. 1).

FRAP is sensitive to changes in botax mobility, which is a function of diffusion, confinement and binding. To understand how fluorescence recovery depends on botax mobility, we consider a first-order botax-binding reaction scheme:

$$\mathrm{botax}_{\mathrm{free}}^{\mathrm{unbleached}} \xleftarrow{k^*} \mathrm{botax}_{\mathrm{free}}^{\mathrm{bleached}} + MT_{\mathrm{empty}} \underset{k_{\mathrm{off}}}{\overset{k_{\mathrm{on}}}{\leftrightarrows}} \mathrm{botax}_{\mathrm{bound}}^{\mathrm{bleached}}$$

where we assume k_{on} and k_{off}, the rates of botax association and dissociation to and from an empty site on the MT interior, are independent of the state of the fluorophore, and k^*, the rate at which free (unbound) bleached botax is replaced by free fluorescent (unbleached) botax in the MT lumen, is irreversible because $\left[\mathrm{botax}_{\mathrm{free}}^{\mathrm{bleached}}\right]$ outside the MT is negligible.Because free botax inside the MT is in equilibrium with botax outside the MT at all times, and because the bleached spot profile, which was approximately gaussian, did not increase in width over time (data not shown), k^* is essentially the rate at which botax passes through the pores in the MT wall, $k^* = k_{\mathrm{out}} = -k_{\mathrm{in}}$.

This manner of characterizing the confinement of botax imposed by the microtubule wall in terms of a rate constant (e.g., k_{out}) is justified only if characteristic time scales extracted from the data are slow compared to the time scale for diffusion across the bleached spot, $t_{\mathrm{diffusion}} = r^2/4D$. Given the diffusion constant of taxol, $D \sim 100\ \mu\mathrm{m}^2/\mathrm{s}$, and the typical bleach spot radius, $r \sim 20\ \mu\mathrm{m}$, in our experiment $t_{\mathrm{diffusion}} \sim 1$ s is indeed two to three orders of magnitude faster than recovery.

Differential equations derived from the reaction scheme above describe how both free and bound concentrations of bleached botax change over time:

$$\frac{\mathrm{d}}{\mathrm{d}t}[\mathrm{botax}_{\mathrm{free}}] = k_{\mathrm{off}}[\mathrm{botax}_{\mathrm{bound}}] - k_{\mathrm{on}}\left[\mathrm{MT}_{\mathrm{empty}}\right][\mathrm{botax}_{\mathrm{free}}] - k_{\mathrm{out}}[\mathrm{pores}][\mathrm{botax}_{\mathrm{free}}] \quad (2)$$

$$\frac{\mathrm{d}}{\mathrm{d}t}[\mathrm{botax}_{\mathrm{bound}}] = -k_{\mathrm{off}}[\mathrm{botax}_{\mathrm{bound}}] + k_{\mathrm{on}}\left[\mathrm{MT}_{\mathrm{empty}}\right][\mathrm{botax}_{\mathrm{free}}] \quad (3)$$

To interpret FRAP, we determine the time course of bound fluorescent botax by solving Eqs. (2) and (3) simultaneously. We simplify the equations by rewriting $[\mathrm{MT}_{\mathrm{empty}}]$ in terms of the concentration of binding sites inside the MT,

$$[\mathrm{sites}] = \frac{\#\beta\text{-tubulin}}{\mathrm{volume}} = \frac{2\pi RL/a}{\pi R^2 L} = \frac{2}{aR}, \quad (4)$$

multiplied by $\langle\xi\rangle$, the proportion of empty binding sites to total binding sites

$$\langle\xi\rangle = \frac{[\mathrm{MT}_{\mathrm{empty}}]}{[\mathrm{MT}_{\mathrm{empty}}] + [\mathrm{botax}_{\mathrm{bound}}]} = \left[1 + \frac{[\mathrm{botax}_{\mathrm{bound}}]}{[\mathrm{MT}_{\mathrm{empty}}]}\right]^{-1} = \left[1 + \frac{[\mathrm{botax}_{\mathrm{free}}]}{K_{\mathrm{D}}}\right]^{-1}, \quad (5)$$

where K_D is the equilibrium dissociation constant for botax binding the MT, R is the microtubule inner radius (~8 nm) and a is the surface area per tubulin dimer (~32 nm^2). We set [pores] equal to [sites] because, although each tubulin dimer creates two pores, it has recently been determined that only one is big enough to allow botax to pass [25]. Thus, Eqs. (2) and (3) become

$$\frac{d}{dt}[\text{botax}_{\text{free}}] = k_{\text{off}}[\text{botax}_{\text{bound}}] - \frac{2}{aR}k_{\text{on}}\langle\xi\rangle[\text{botax}_{\text{free}}] - \frac{2}{aR}k_{\text{out}}[\text{botax}_{\text{free}}] \quad (2')$$

$$\frac{d}{dt}[\text{botax}_{\text{bound}}] = -k_{\text{off}}[\text{botax}_{\text{bound}}] + \frac{2}{aR}k_{\text{on}}\langle\xi\rangle[\text{botax}_{\text{free}}] \quad (3')$$

Their solution is straightforward (see Supplementary material) using Laplace transforms and assuming (i) [botax$_{\text{bound}}$] follows a simple exponential decay and (ii) equilibration across the MT wall is relatively fast, $2k_{\text{out}}/aR \gg 1/\tau_R$. Assumption (i) is consistent with our observations. Assumption (ii) is justified by the high density of pores along the MT wall ($\geqslant$10 mM), which allows botax to escape the lumen faster than the fastest recovery time.

The resulting characteristic time for recovery of bound bleached botax depends on the reaction rates and the proportion of empty binding sites as

$$\tau_R \approx k_{\text{off}}^{-1}\left(1 + \frac{k_{\text{on}}}{k_{\text{out}}}\langle\xi\rangle\right) \quad (6)$$

Note that, as expected, recovery is fastest at high concentrations of free botax, when sites are fully occupied (i.e., $\langle\xi\rangle \to 0$). In this case, dissociation is the rate-limiting step. In the opposite limit (i.e., $\langle\xi\rangle \to 1$), sites are rarely occupied and the time for recovery depends on the relative rates for binding and escaping, as given by the ratio $k_{\text{on}}/k_{\text{out}}$. If $k_{\text{on}} >> k_{\text{out}}$, bleached molecules that dissociate from a taxol-binding site are likely to rebind before re-equilibrating with fluorescent botax in solution, making recovery slower. If $k_{\text{on}} << k_{\text{out}}$, bleached molecules are replaced by unbleached molecules before they have a chance to rebind, making recovery faster.

Botax mobility in the high- and low-concentration regimes

Recovery times of botax in the absence of tau range from 250 to 1000 s as total botax concentration decreases (Fig. 3A).

In the limit of high botax concentrations, recovery is rate-limited by dissociation from MTs. Accordingly, at $\geqslant$1 μM free botax concentration, the recovery time is ~250 s for all conditions tested (Fig. 3) and its inverse measures the microscopic dissociation rate of botax, $k_{\text{off}} \approx 4 \times 10^{-3}$ s^{-1}. This dissociation rate is similar to that of another fluorescent taxol, Flutax-1, $k_{\text{off}} \approx 5 \times 10^{-3}$ s^{-1}, as measured by fluorescence anisotropy [26].

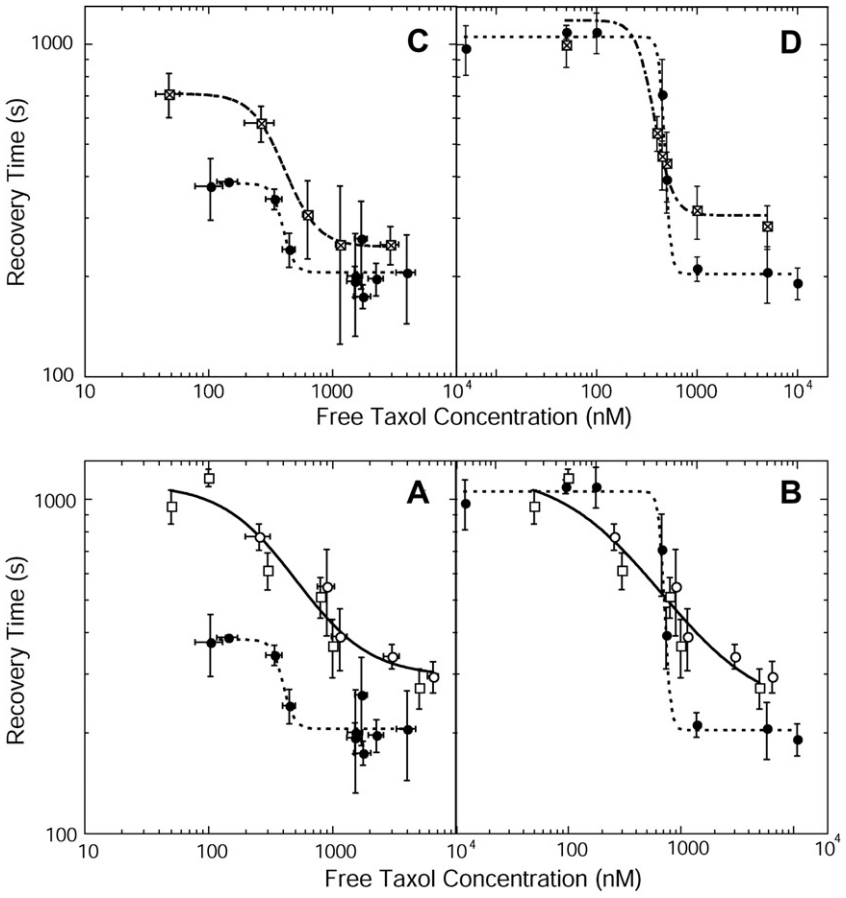

Fig. 3. Recovery time for botax fluorescence on microtubule bundles was measured as function of free botax concentration. Recovery time is affected differently by 3rTau (A and C) and 4rTau (B and D) at the lowest concentrations of free botax but unaffected at the highest concentrations. Data taken at a molar ratio of 1:1 Tau:tubulin (filled symbols) are compared with data taken in the absence of tau (A and B: open symbols) and at intermediate molar ratios of 1:3 of 3rTau:tubulin and 1:10 4rTau:tubulin (C and D: crossed symbols). Data represented as squares are reproduced from. Curves are least squares fits to the kinetic model, Eq. (7), discussed in the text. Fit parameters are listed in Table 1.

Table 1
Kinetic constants of dissociation (k_{off}) passage (k_{out}) and Effective dissociation constant (K_D^*) for botax binding to microtubule

	No Tau	3-Repeat Tau:Tubulin		4-Repeat Tau:Tubulin[a]	
		1:3	1:1	1:10	1:1
	1	1	1	1	1
k_{off} (s^{-1})	294 ± 79	245 ± 6	205 ± 11	305 ± 113	203 ± 28
k_{out} (10^3 M^{-1} s^{-1})	5.6 ± 1.4	9.8 ± 0.2	26.0 ± 3.0	5.2 ± 1.0	5.3 ± 0.2
n_H	1.5 ± 0.7	3.3 ± 0.2	9.6 ± 5.0	4.9 ± 8.2	15.5 ± 3.9
K_D^* (nM)	330 ± 125	355 ± 10	391 ± 30	332 ± 138	461 ± 7

[a] Data from Ref. [16] fit with Eq. (7).

As botax concentration decreases, the recovery time increases. However, instead of increasing monotonically, as would be expected in a diffusion-limited regime, at ⩽100 nM free botax concentration, the recovery time is ~1000 s independent of concentration. In this regime, recovery is rate-limited by rebinding, rather than diffusion. That is 4 times slower than dissociation implies that taxol rebinds ~4 times before it escapes though the pores in the MT wall and constrains the ratio of k_{on}/k_{out} in our model.

A Hill coefficient is needed to capture sensitivity to botax concentration in the presence of Tau

The model summarized in Eq. (5) fits the data only in the absence of tau. As previously observed for 4rTau [16], the presence of 3rTau causes the recovery time to become sensitive to taxol concentration. To fit the data, it suffices to introduce a Hill coefficient, n_H, in the dependence of $\langle\xi\rangle$ on taxol concentration [27]

$$\tau_R^* \approx k_{off}^{-1}\left(1+\frac{k_{on}}{k_{out}}\left(1+\left(\frac{[\text{botax}_{free}]}{K_D^*}\right)^{n_H}\right)^{-1}\right) \quad (7)$$

All data were fitted with Eq. (6) and parameters k_{off}, k_{out}, K_D^* and n_H are listed in Table 1.

Although this functional form is empirical, the fitted parameters provide clues to help inform further modeling. First, in the absence of tau, fitting with Eq. (6) yields a Hill coefficient consistent with n_H ~1, indicating that cooperativity is weak or non-existent on bare MTs. Second, the Hill coefficient increases as the concentration of either tau isoform increases, although not as much in the case of 3rTau as compared to 4rTau. Third, both the dissociation rate, k_{off}, and the effective dissociation constant, K_D^*, are similar in all cases. The latter is especially interesting because the fitted value, $K_D^* \sim 300$ nM differs markedly from that of the equilibrium dissociation constant, $K_D \sim 2$ μM. More elaborate modeling is needed to explain this discrepancy. We defer this to future work and focus here on isoform-dependent effects.

Tau isoform dependence on taxol mobility

Tau isoforms have either three or four conserved peptide repeats (R1, R2, R3 and R4) in their C-terminal domain. 3rTau isoforms lack R2 and the region that separates it from R1 [19]. As a result, their MT-binding affinity is ~3-fold less than that of 4rTau isoforms (~0.1 μM) [9]. We therefore made measurements with 3rTau at a molar ratio of 1:3 tau:tubulin for comparison to measurements made with 4rTau at a molar ratio of 1:10 tau:tubulin [16]. Under our reaction conditions (>10 μM tubulin) such molar ratios are expected to fully saturate the MTs with tau [28]. However, it is known that over-saturating levels of tau continue to bind MTs [29,30] and botax mobility in the presence of a 1:1 molar ratio of 4rTau:tubulin is strikingly different than in the presence of a 1:10 molar ratio [16]. Therefore, we made measurements with 3rTau at a molar ratio of 1:1 tau:tubulin, as well.

The effects of 3rTau and 4rTau on botax mobility are compared in Fig. 3. At high concentrations of free botax, the recovery time, τ_R ~250 s, is the same with or without either 3rTau or 4rTau. Thus, dissociation of botax is unaffected by either tau isoform. In the absence of tau, as botax concentration decreases, the increase in τ_R is gradual, but in the presence of either 3rTau or 4rTau, it becomes sensitive to free botax concentration around 300 nM. The sensitivity is greater at the higher molar ratio of tau:tubulin for both isoforms (Fig. 3C and D), but much more so in the case of 4rTau.

The most remarkable difference in the effects of 3rTau and 4rTau occurs at low botax concentrations. In this regime, botax recovery in the presence of 4rTau is as slow as in the absence of tau (~1000 s) but recovery in the presence of 3rTau at a 1:1 molar ratio with tubulin is nearly 2.5 times faster (~450 s) (Fig. 3A and B). Measurements at a 1:3 molar ratio indicated that this effect is a function of 3rTau concentration, and were therefore repeated at molar ratios ranging from 1:100 to 1:1 with 100 nM free botax concentration (Fig. 4). The effect was first detected at a 1:10 molar ratio and becomes more pronounced upon further addition of 3rTau. This onset is well above the physiological molar ratio of tau to tubulin (~1:17 as measured in PC12 neurons [31]).

Mechanisms of fast recovery

In the low botax concentration regime, recovery is rate-limited by the concentration-independent relative probabilities for rebinding versus escaping the MT lumen. The most dramatic isoform-dependent effect is seen in this regime. In either the absence of

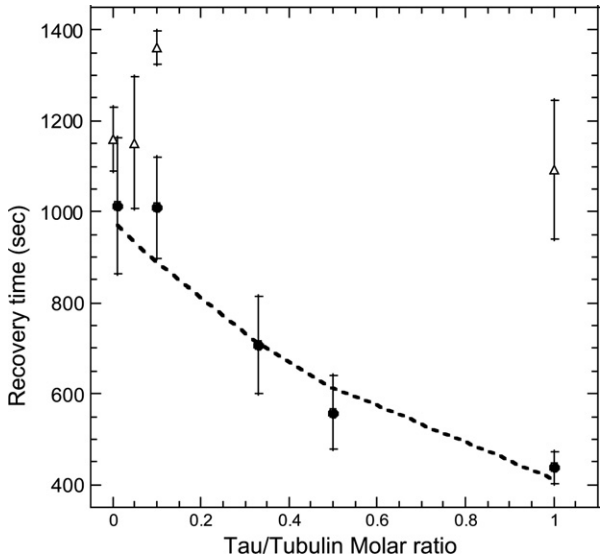

Fig. 4. Recovery time of botax on MT bundle was measured as a function of 3r or 4rTau to tubulin ratio from 0:1 to 1:1 at 100 nM free botax concentration (3rTau: filled circle, 4rTau: open triangle). The dashed line represents the recovery time when 3rTau binds to taxol site with botax on MTs with 1 μM binding affinity ($K_D^{Tau^*}$).

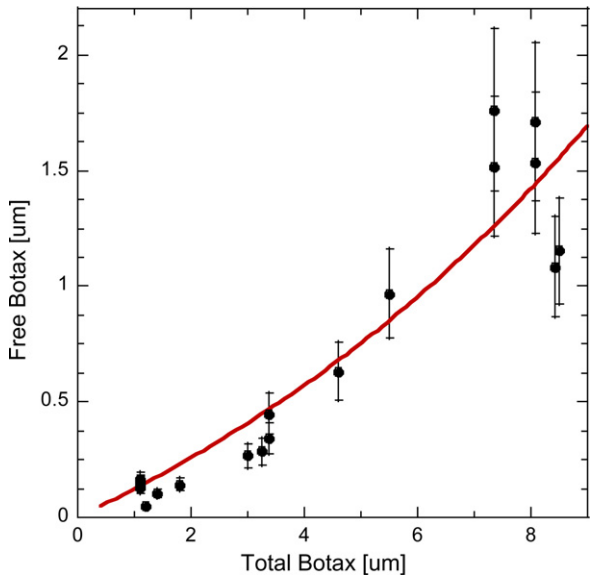

Fig. 5. Measurement of botax-binding affinity, K_D, for microtubules (MTs) as measured by the free botax concentration that resulted from different total concentrations of botax added. Data taken in the absence of tau, 1:3 3rTau:tubulin and 1:1 3rTau:tubulin are fit together using the function $K_D \equiv [MT_{empty}][botax_{free}]/[botax_{bound}] = (f \times [tubulin_{total}] - [(botax_{total} - botax_{free})])[botax_{free}]/[botax_{total} - botax_{free}]$, with f as polymerization rate 0.95 and K_D as the only free parameter. Solid lines are least-squares best fits yielding $K_D = 2.3\ \mu M \pm 0.2$.

tau or the presence of 1:1 4rTau:tubulin, recovery takes four times longer than dissociation. In the presence of 1:1 3rTau:tubulin, it is much faster—only about two dissociation times. Thus, 3rTau greatly reduces the probability for botax rebinding.

We consider three possible mechanisms to explain fast recovery at low botax concentrations: (i) 3rTau decreases the botax-binding affinity of botax; (ii) 3rTau competes with botax for its binding site on the MT; (iii) 3rTau changes the MT structure so as to increase k_{out}.

(i) Affinity of botax for microtubule is unaffected by Tau

Given that k_{off} is unaffected by tau (Fig. 3), if 3rTau speeds recovery by altering botax affinity, it must decrease k_{on} (Eq. (6)). For example, to explain the measured 450 s recovery time at 100 nM free botax with a 1:1 ratio of 3rTau:tubulin by a change in botax affinity, implies $K_D = 10\ \mu M$—a 4-fold reduction.

We used fluorimetry under the microscope to quantify free botax and determine whether botax affinity was changed by 3rTau (see Materials and methods). We found $K_D = 2.3 \pm 0.2\ \mu M$ (Fig. 5), the same as measured in bulk on GDP-tubulin in either the absence or the presence of 4rTau [16]. This result is also consistent with stopped-flow experiments, which found 4rTau does not alter taxol kinetics [32].

We therefore exclude changes in affinity as a possible explanation for the fast recovery observed in the presence of 3rTau.

(ii) 3rTau may compete for taxol-binding sites

The presence of 3rTau could speed recovery by binding directly to the botax-binding site, decreasing the number of available binding sites and thereby decreasing the probability of botax rebinding.

The possibility that 3rTau competes for taxol-binding sites is suggested by two recent results. It has been shown that a saturating concentration of taxol can reduce the amount of bound tau—an effect that is more pronounced for 3rTau than 4rTau [13]. It has also been observed that taxol induces tau detachment from MTs when tau is highly expressed *in vivo* [17]. Both results imply that tau loses to taxol in a competition for MT binding sites.

Our data show that recovery time decreases gradually as the molar ratio of 3rTau to tubulin increases [4]. In the competition scenario, the corresponding decrease in the proportion of available binding sites $\langle \xi \rangle$ at each molar ratio of tau to tubulin can be quantified by comparison with recovery times measured in the absence of tau (Fig. 3A).

If 3rTau competes for taxol binding sites, we can write down equilibrium equations for botax and tau binding to either outer and/or inner sites on the MTs, respectively.

$$K_D^{botax} = \frac{\left([sites] - [botax_{bound}] - \left[Tau_{bound}^{inner}\right]\right) \cdot ([botax_{total}] - [botax_{bound}])}{[botax_{bound}]} \tag{8}$$

$$K_D^{Tau} = \frac{([sites] - [Tau_{bound}^{outer}]) \cdot \left([Tau_{total}] - [Tau_{bound}^{outer}] - \left[Tau_{bound}^{inner}\right]\right)}{[Tau_{bound}^{outer}]} \tag{9}$$

$$K_D^{Tau^*} = \frac{\left([sites] - [botax_{bound}] - \left[Tau_{bound}^{inner}\right]\right) \cdot \left([Tau_{total}] - [Tau_{bound}^{outer}] - \left[Tau_{bound}^{inner}\right]\right)}{\left[Tau_{bound}^{inner}\right]} \tag{10}$$

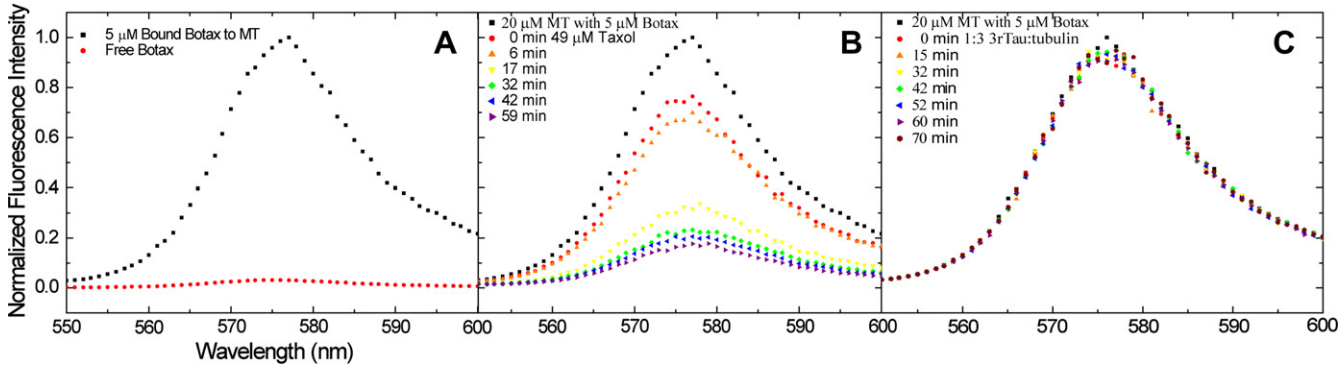

Fig. 6. (A) Comparison of fluorescence emission spectra of botax free in solution (dotted line, 5 μM botax) and fully bound to microtubules (dashed line, 5 μM botax with 20 μM tubulin); (B and C) Time series of fluorescence emission spectra of botax on microtubules following the addition of either (B) unlabeled taxol (48 μM final concentration) or (C) 3rTau (1:3 final molar ratio with tubulin).

In Eqs. (9) and (10), we assume that one 3rTau only binds either to the outside of the MT or to the taxol-binding site in MT lumen. The bulk affinities of botax for the taxol site and tau for the outside of the MT are known (K_D^{botax} ~2.3 μM and K_D^{Tau} ~0.3 μM)[9]. Using these values, we tested various affinities ($K_D^{Tau^*}$) of 3rTau for the taxol site to solve Eqs. (8)–(10) simultaneously and compared the predicted occupancy of inner sites, $([botax_{bound}] + [Tau^{inner}_{bound}])/[sites] = 1 - \langle\xi\rangle$, with the one implied by the recovery time at each 3rTau concentration for the case of 100 nM free botax. The best fit to the data (dashed line in Fig. 4), as measured by the RMS standard deviation of the errors, occurs with $K_D^{Tau^*} \sim 1$ μM, although the quality of the fit would benefit from more elaborate modeling.

We sought further evidence of competition by fluorimetry. If 3rTau binds to the taxol site, it would displace botax and then leads to a decrease in fluorescence. Based on the $K_D^{Tau^*} \sim 1$ μM suggested above, the increase in free botax concentration expected upon adding a 1:1 ratio of tau to MTs in 100 nM of free botax is only 6%, well below our sensitivity (~26%) under the microscope. We therefore performed a direct competition for taxol sites, first verifying our approach using paclitaxel, a ligand similar to botax but without the fluorescent label. Addition of paclitaxel reduced the peak fluorescence intensity of botax at equilibrium as expected (see Supplementary material) (Fig. 6B). Addition of a 1:3 3rTau:tubulin ratio to botax-bound MTs resulted in no perceptible reduction (<10%) of fluorescence (Fig. 6C). This observation reinforces the absence of any effect on botax affinity, discussed in connection with mechanism (i). However, limitations on the quantity of 3rTau, combined with intensity demands of the fluorimeter make for a relatively weak constraint on competition, $K_D^{Tau^*} > 10$ nM, consistent with the results above.

(iii) Tau stabilizes tube structure, but it may change pores

A third possible mechanism by which 3rTau could speed recovery would be if it induces a structural change in the MT that increases in k_{out}, the rate at which taxol escapes the MT lumen.

It is well known that taxol can cause open MTs to form [33]. To see whether 3rTau also causes open tubes, we looked by TEM at cross sections of MTs that were prepared in the same way as for FRAP (Fig. 7). For all conditions, over 90% of MTs were in closed tube form. The small numbers of imperfect MTs could be classified as hooked tubes, open tubes or bowties. The presence of both 3rTau and 4rTau reduced the number of hooked and opened tubes.

To be sure the TEM preparation itself was not biasing the results, we verified that at a high concentration of botax (136 μM botax and 22.7 μM tubulin), more than 30% of MTs were open tubes. We noticed, however, that even at such a high botax concentrations, if saturating levels of 4rTau were present before the addition of taxol, <5% of MTs were open tubes (data not shown). Thus, both isoforms of tau suppress the formation of open MT structures, and 4rTau can do so even under conditions that otherwise support a large number of open structures.

This result indicates that, if 3rTau causes a structural change that enhances the rate at which luminal botax exchanges with bulk botax, it is doing so at the pores, rather than on the tube as a whole.

There are few experimental trials to look the detail of the pores in the absence or presence of ligands by cryo-EM and AFM. In absence of MAPs, only one among two types of pore has a similar size with taxol ligand for diffusion. It suggests that 3rTau may increase the pores and make passage faster [25,26,34]. But, structural change in the pores by tau binding is inconclusive. Tau mainly binds along protofilaments on MT exterior that there is no significant change in the valley between protofilaments where the pore exists [11,30]. At over-saturating concentration of tau, however, tau forms dimer or oligomerization on MT surface [29,35]. This

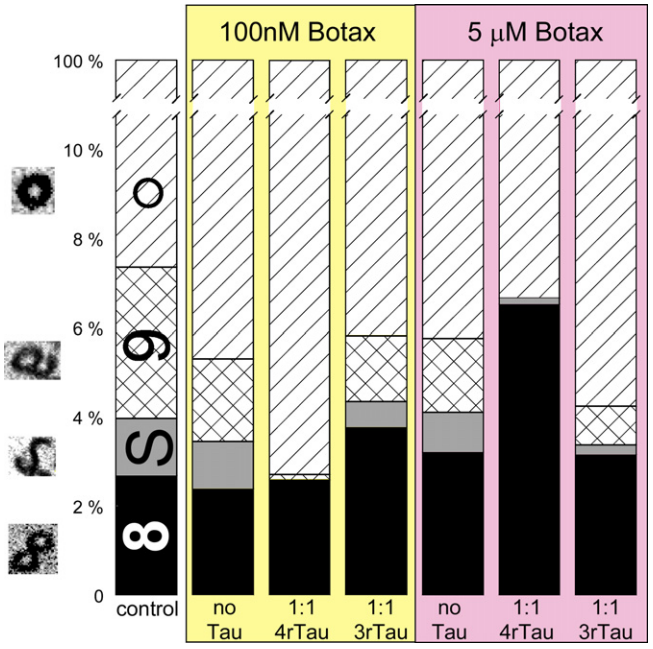

Fig. 7. Structure of MTs polymerized with no botax and no Tau as control, with no tau and either 1:1 ratio of 3rTau or 4rTau in the presence of 100 nM botax (4% sites are filled: yellow box) and with no tau and either 1:1 ratio of 3rTau or 4rTau in the presence of 5 μM botax (70% filled: purple box), were classified as closed tubes (O), hooks (σ), opened tube (S) or bowties (∞). Pictures on the left side of graph were taken under transmission electron microscopy at 80 kV. Number of MTs counted was >800 for each condition. (For interpretation of the references to color in this figure legend, the reader is referred to the web version of this paper.)

clustering may interfere with taxol penetration but has been poorly solved yet.

Besides the size of pore, we also considered the pore affinity since taxol's outer site has been revealed [32,36]. In study of Buey et al., taxol binds to a site near the pore on MT exterior and then reaches a kinetically unfavorable luminal site. The pathway of taxol translocation is unknown, but this rate of this is same as k_{out} in our model. Thus, if 3rTau decreases the affinity of outer sites, the passage rate increases. Structural studies elaborating on the complex of MT with tau and taxol that reveal the size or affinity of pores would be able to elucidate this mechanism.

Conclusions

There exists a dramatic isoform-dependent effect on botax mobility among MTs at low botax concentrations. 3rTau suppresses botax rebinding, whereas 4rTau has no effect. 3rTau does not alter the affinity of botax for its binding site, however, so its effect on rebinding must be explained either by it competing for the botax-binding site, or by it inducing a structural change in the MT wall. Current experiments cannot rule out both mechanisms, but their plausibility are diminished by the fact that 4rTau which has no effect on rebinding. Because 4rTau has all the same binding sites with 3rTau, the inserted peptides in 4rTau, which is lack in 3rTau and the strongest binding region to MTs, may a key region for isoforms dependent manner including dynamic instability, structural changes and interacting with luminal side of MTs.

Acknowledgments

We thank Dr. Stuart Feinstein (University of California, Santa Barbara) for the gift of Tau and Dr. Yong-Seok Jho for discussions of modeling. This work was supported by a grant from the Basic

Atomic Energy Research Institute (BAERI) program funded by the Ministry of Science and Technology of Korea (MOST), the Korea Health 21 R&D Project by Ministry of Health and Welfare, US National Science Foundation Faculty Early Career Development (CAREER) Program Award BIO99-85493 and the IMI program of the National Science Foundation under Award No. DMR04-09848.

Appendix A. Supplementary data

Supplementary data associated with this article can be found, in the online version, at doi:10.1016/j.abb.2008.07.020.

References

[1] J.S.L. Hyams, C.W. Microtubules, Modern Cell Biology, Wiley-Liss, New York, 1994.
[2] R.B. Maccioni, V. Cambiazo, Physiol. Rev. 75 (1995) 835–864.
[3] M.G. Spillantini, M. Goedert, Trends Neurosci. 21 (1998) 428–433.
[4] K.S. Kosik, C.L. Joachim, D.J. Selkoe, Proc. Natl. Acad. Sci. USA 83 (1986) 4044–4048.
[5] M. Goedert, M.G. Spillantini, R. Jakes, D. Rutherford, R.A. Crowther, Neuron 3 (1989) 519–526.
[6] O. Schweers, E. Schonbrunn-Hanebeck, A. Marx, E. Mandelkow, J. Biol. Chem. 269 (1994) 24290–24297.
[7] S. Jeganathan, M. von Bergen, H. Brutlach, H.J. Steinhoff, E. Mandelkow, Biochemistry 45 (2006) 2283–2293.
[8] N. Hirokawa, Y. Shiomura, S. Okabe, J. Cell Biol. 107 (1988) 1449–1459.
[9] B.L. Goode, M. Chau, P.E. Denis, S.C. Feinstein, J. Biol. Chem. 275 (2000) 38182–38189.
[10] M.F. Chau, M.J. Radeke, C. de Ines, I. Barasoain, L.A. Kohlstaedt, S.C. Feinstein, Biochemistry 37 (1998) 17692–17703.
[11] J. Al-Bassam, R.S. Ozer, D. Safer, S. Halpain, R.A. Milligan, J. Cell Biol. 157 (2002) 1187–1196.
[12] R.A. Santarella, G. Skiniotis, K.N. Goldie, P. Tittmann, H. Gross, E.M. Mandelkow, E. Mandelkow, A. Hoenger, J. Mol. Biol. 339 (2004) 539–553.
[13] S. Kar, J. Fan, M.J. Smith, M. Goedert, L.A. Amos, EMBO J. 22 (2003) 70–77.
[14] M.A. Jordan, L. Wilson, Methods Enzymol. 298 (1998) 252–276.
[15] E.K. Rowinsky, Semin. Oncol. 24 (1997) S19-1–S19-12.
[16] J.L. Ross, C.D. Santangelo, V. Makrides, D.K. Fygenson, Proc. Natl. Acad. Sci. USA 101 (2004) 12910–12915.
[17] A. Samsonov, J.Z. Yu, M. Rasenick, S.V. Popov, J. Cell Sci. 117 (2004) 6129–6141.
[18] B. Zhang, A. Maiti, S. Shively, F. Lakhani, G. McDonald-Jones, J. Bruce, E.B. Lee, S.X. Xie, S. Joyce, C. Li, P.M. Toleikis, V.M. Lee, J.Q. Trojanowski, Proc. Natl. Acad. Sci. USA 102 (2005) 227–231.
[19] D. Panda, J.C. Samuel, M. Massie, S.C. Feinstein, L. Wilson, Proc. Natl. Acad. Sci. USA 100 (2003) 9548–9553.
[20] J.M. Bunker, L. Wilson, M.A. Jordan, S.C. Feinstein, Mol. Biol. Cell 15 (2004) 2720–2728.
[21] W. Herzog, K. Weber, Eur. J. Biochem. 91 (1978) 249–254.
[22] J.L. Ross, D.K. Fygenson, Biophys. J. 84 (2003) 3959–3967.
[23] J. Chen, Y. Kanai, N.J. Cowan, N. Hirokawa, Nature 360 (1992) 674–677.
[24] R. Mukhopadhyay, J.H. Hoh, FEBS Lett. 505 (2001) 374–378.
[25] A. Krebs, K.N. Goldie, A. Hoenger, EMBO Rep. 6 (2005) 227–232.
[26] J.F. Diaz, I. Barasoain, J.M. Andreu, J. Biol. Chem. 278 (2003) 8407–8419.
[27] T.L. Hill, Cooperativity Theory in Biochemistry, Springer, New York, 1985.
[28] S.F. Levy, A.C. Leboeuf, M.R. Massie, M.A. Jordan, L. Wilson, S.C. Feinstein, J. Biol. Chem. 280 (2005) 13520–13528.
[29] M. Ackmann, H. Wiech, E. Mandelkow, J. Biol. Chem. 275 (2000) 30335–30343.
[30] I.A. Schaap, B. Hoffmann, C. Carrasco, R. Merkel, C.F. Schmidt, J. Struct. Biol. 158 (2007) 282–292.
[31] D.G. Drubin, S.C. Feinstein, E.M. Shooter, M.W. Kirschner, J. Cell Biol. 101 (1985) 1799–1807.
[32] J.F. Diaz, I. Barasoain, A.A. Souto, F. Amat-Guerri, J.M. Andreu, J. Biol. Chem. 280 (2005) 3928–3937.
[33] E. Hamel, A.A. del Campo, M.C. Lowe, C.M. Lin, J. Biol. Chem. 256 (1981) 11887–11894.
[34] H. Li, D.J. DeRosier, W.V. Nicholson, E. Nogales, K.H. Downing, Structure (Camb.) 10 (2002) 1317–1328.
[35] V. Makrides, T.E. Shen, R. Bhatia, B.L. Smith, J. Thimm, R. Lal, S.C. Feinstein, J. Biol. Chem. 278 (2003) 33298–33304.
[36] R.M. Buey, E. Calvo, I. Barasoain, O. Pineda, M.C. Edler, R. Matesanz, G. Cerezo, C.D. Vanderwal, B.W. Day, E.J. Sorensen, J.A. Lopez, J.M. Andreu, E. Hamel, J.F. Diaz, Nat. Chem. Biol. 3 (2007) 117–125.